# Interaction between a single photon and a weak coherent state mediated by a quantum emitter

Dat Thanh Le (Brisbane, Australia)

Nguyen Ba An (Hanoi, Vietnam)

(Received Sept. 24, 2025; accepted Oct. 30, 2025)

Abstract. Photon-photon interaction, an essential ingredient for optical quantum technologies, is indirect actually, i.e., often mediated via a nonlinear medium. In this work, we consider a single photon interacting with a weak coherent state in a one-dimensional waveguide coupled to a two-level quantum emitter. We present a general input-output framework that applies to an arbitrary input Fock state and various types of quantum emitters. We then use this to compute the relevant scattering processes between the single photon and the weak coherent state. We analyse in detail the characteristics of the output state taking into account the continuous-mode nature of the input and output states which are treated as appropriate photon wavepackets.

#### 1. Introduction

Single photons, despite being ideal carriers of quantum information with low decoherence and ease of transmission, hardly interact with each other, which introduces a major bottleneck in implementing two-qubit gates needed for universal quantum computation [1, 2]. Interaction and manipulation at the single-photon level are thus mostly indirect, relying on measurement-induced

 $Key\ words\ and\ phrases$ : Waveguide quantum electrodynamics, quantum emiiters, photon-photon interaction.

 $2020\ Mathematics\ Subject\ Classification :\ 81\text{U}10,\ 81\text{U}20$ 

nonlinearity [3, 4] or a mediate nonlinear medium [5, 6]. The emerging field of waveguide quantum electrodynamics (QED) follows the latter approach, where photons interact with localised quantum emitters embedded in one-dimensional (1D) waveguides. Physical platforms to implement waveguide QED primarily include ultracold atoms trapped in optical fibers [7, 8], quantum dots embedded in photonic crystal waveguides [9, 10], and superconducting qubits coupled to transmission lines [11, 12]. In these systems, due to the confined dimensions quantum emitters couple strongly to only a few propagating photon modes [13], which can lead to strong effective photon-photon interaction [14]. Harnessing this effect, single-photon transistors [15], switches [16], and quantum nonlinear optics with single photons [17, 18] have been demonstrated.

Photon scattering processes are central to the studies of waveguide QED, most of which have so far considered scattering of either Fock states [19, 20, 21, 22, 23, 24] or coherent states [25, 26] but not a pair of input states of both types. However, interaction between a single photon and a coherent state is of potential use in optical quantum technologies. In particular, via a weak cross-Kerr medium a single photon could impart a detectable phase shift on a strong coherent state. This effect can be exploited to implement nondemolition photon-number detection and controlled-phase gates between individual photons [27, 28]. Despite initial criticism due to an idealised single-mode quantum treatment of the cross-phase modulation [29, 30, 31], it was shown in Refs. [32, 33] using a general theory of continuous-mode photonic pulses that such cross-Kerr scheme can achieve high fidelity, provided that the input pulses fully pass through each other. In addition, single photons and coherent states can be combined to construct hybrid discrete-continuous qubits [34, 35]. This hybrid approach to optical quantum information processing can outperform its discrete and continuous counterparts in various quantum tasks [36, 37, 38].

In this paper, we study the interaction between a single-photon state  $|1\rangle$  and a coherent state  $|\eta\rangle$  in a 1D waveguide coupled to a two-level emitter. The two input states are necessarily in orthogonal modes, for example, with respect to polarisation or spatial modes, so that they can be treated independently in a mutual form of a product state. As light-emitter interaction is of dipole coupling nature [39] (i.e.,  $\hat{H}_{\rm int} \propto -\hat{\mathbf{d}}.\hat{\mathbf{E}}$  with  $\hat{\mathbf{d}}$  the emitter's electric dipole and  $\hat{\mathbf{E}}$  the field operator), the photons interact significantly with the emitter only when their polarisation aligns with that of the two-level atom's only transition  $(|g\rangle\leftrightarrow|e\rangle$ , with  $|g\rangle$  and  $|e\rangle$  the emitter's ground and excited states). Therefore, in our analysis the input single photon and the input coherent state have the same polarisation set by the two-level emitter but counter-propagate to each other, as shown in Fig. 1. Furthermore, we consider the coherent state with a small amplitude (i.e., with  $\eta$  such that  $|\eta|^2 \ll 1$ ) to avoid unwanted saturation effects on the emitter due to strong coherent drives in realistic experiments [40]. This also simplifies the relevant scattering calculations.

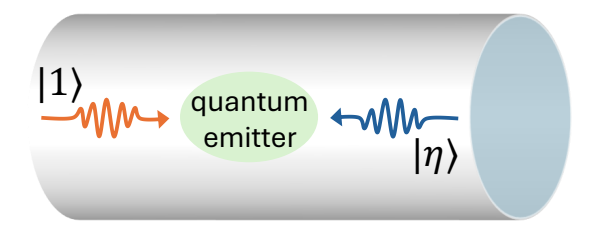


Figure 1: Diagram of a single photon  $|1\rangle$  and a coherent state  $|\eta\rangle$  counterpropagating in a non-chiral 1D waveguide coupled a general quantum emitter. In our work, the emitter is chosen to be a two-level atom with a transition frequency  $\Omega$ .

We organise this work as follows. In Section 2, we introduce a generalised input-output formalism that computes the scattering of input states with an arbitrary photon number [22, 41], with discrete examples applied for one- and two-photon scatterings. We then address the interaction between a single-photon state and a coherent state in Section 3. Using Fock-state representation of a weak coherent state  $|\eta\rangle \simeq c_0|0\rangle + c_1|1\rangle$  with proper coefficients  $c_0$  and  $c_1$  for  $|\eta|^2 << 1$ , the interested scattering scenario is well reduced to sum of two processes: one is single-photon scattering due to the term  $c_0|0\rangle|1\rangle$  and the other is two-photon one due to the term  $c_1|1\rangle|1\rangle$ . We then use the input-output formalism introduced in Section 2 to compute the output state. Based on this, we numerically analyse the characteristics of the output state, including its fidelity to the ideal phase-shifted output state and its photon distribution. We conclude our work in Section 4 and include Appendix A and Appendix B to complement the results in the main text.

# 2. Generalised input-output formalism

# 2.1. Hamiltonians and input-output relation

We consider a localised quantum emitter coupled to a non-chiral (i.e., two-mode) waveguide. The total Hamiltonian for this setup is given by

$$\hat{H} = \hat{H}_{\text{emi}} + \hat{H}_{\text{wg}} + \hat{H}_{\text{int}},$$

where  $\hat{H}_{\rm emi}$  (to be specified later) is the emitter Hamiltonian,  $\hat{H}_{\rm wg}$  is the waveguide Hamiltonian, and  $\hat{H}_{\rm int}$  is the emitter-waveguide interaction Hamiltonian.

The latter two are given by

(2.2) 
$$\hat{H}_{\text{wg}} = \sum_{\alpha} \int_{-\infty}^{\infty} d\omega \omega \hat{b}_{\alpha}^{\dagger}(\omega) \hat{b}_{\alpha}(\omega),$$

(2.3) 
$$\hat{H}_{\text{int}} = i \sum_{\alpha} \sqrt{\frac{\gamma_{\alpha}}{2\pi}} \int_{-\infty}^{\infty} d\omega (\hat{b}_{\alpha}^{\dagger}(\omega)\hat{c} - \hat{c}^{\dagger}\hat{b}_{\alpha}(\omega)).$$

In Eqs. (2.2) and (2.3),  $\alpha \in \{r, l\}$  denotes right-moving and left-moving modes,  $\hat{b}_{\alpha}(\omega)$  and  $\hat{b}_{\alpha}^{\dagger}(\omega)$  are waveguide bosonic operators with the commutation relation  $[\hat{b}_{\alpha}(\omega), \hat{b}_{\alpha'}^{\dagger}(\omega')] = \delta_{\alpha,\alpha'}\delta(\omega - \omega')$ ,  $\hat{c}$  and  $\hat{c}^{\dagger}$  (to be specified later) are emitter operators that couple to the waveguide, and  $\gamma_{\alpha}$  is the emitter-waveguide coupling strength. For a non-chiral waveguide, both propagating directions,  $\alpha = r$  or  $\alpha = l$ , are equivalent such that  $\gamma_r \equiv \gamma_l = \gamma$ , i.e., there is only one coupling strength  $\gamma$ . However, in the expression of  $\hat{H}_{\rm int}$  we include  $\gamma_r$  and  $\gamma_l$  as if they are different in general, which is useful in recovering the chiral (or one-mode) waveguide case by setting either  $\gamma_r$  or  $\gamma_l$  to zero.

We note that in deriving the interaction  $H_{\rm int}$  the rotating wave approximation was utilised to remove counter-rotating terms as well as Markov approximation to simplify the coupling strength  $\gamma_{\alpha}$  as independent of  $\omega$  [42]. Another idealisation is that the waveguide frequency range was extended to  $(-\infty, +\infty)$ , which does not affect the total system's dynamics that is only significant in a narrow bandwidth centred around the emitter's transition frequency [43]. Also, in this paper we set  $\hbar=1$  for convenience.

We define the input and output fields for both right- and left-moving modes

(2.4a) 
$$\hat{b}_{\alpha,\text{in}}(t) = \frac{1}{\sqrt{2\pi}} \int d\omega e^{-i\omega(t-t_0)} \hat{b}_{\alpha}(\omega, t_0),$$

(2.4b) 
$$\hat{b}_{\alpha,\text{out}}(t) = \frac{1}{\sqrt{2\pi}} \int d\omega e^{-i\omega(t-t_1)} \hat{b}_{\alpha}(\omega, t_1),$$

where  $t_0$  and  $t_1$  are the initial time in a distant past and the final time in a distant future, respectively. The input and output fields obey the commutation relations

$$(2.5a) \quad \left[\hat{b}_{\alpha,\text{in}}(t), \hat{b}_{\alpha',\text{in}}^{\dagger}(t')\right] = \left[\hat{b}_{\alpha,\text{out}}(t), \hat{b}_{\alpha',\text{out}}^{\dagger}(t')\right] \quad = \quad \delta_{\alpha,\alpha'}\delta(t-t'),$$

$$(2.5b) \quad \left[\hat{b}_{\alpha,\mathrm{in}}(t),\hat{b}_{\alpha',\mathrm{in}}(t')\right] = \left[\hat{b}_{\alpha,\mathrm{out}}(t),\hat{b}_{\alpha',\mathrm{out}}(t')\right] \quad = \quad 0,$$

and are related to each other via the response by the emitter [43]

(2.6) 
$$\hat{b}_{\alpha,\text{out}}(t) = \hat{b}_{\alpha,\text{in}}(t) + \sqrt{\gamma_{\alpha}}\hat{c}(t).$$

Here  $\hat{c}(t) = e^{i\hat{H}t}\hat{c}e^{-i\hat{H}t}$  is a Heisenberg operator, with  $\hat{H}$  given in Eq. (2.1). Furthermore, given an arbitrary emitter operator  $\hat{s}$  we can prove the following

causality relations [43, 44]

$$(2.7a) \qquad \left[ \hat{s}(t), \hat{b}_{\alpha, \text{in}}(t') \right] = \left[ \hat{s}(t), \hat{b}_{\alpha, \text{in}}^{\dagger}(t') \right] = 0 \quad \text{for } t < t',$$

$$\left[\hat{s}(t),\hat{b}_{\alpha,\mathrm{out}}(t')\right] = \left[\hat{s}(t),\hat{b}_{\alpha,\mathrm{out}}^{\dagger}(t')\right] = 0 \quad \text{for } t > t'.$$

Equations (2.7a) and (2.7b), respectively, indicate that the dynamics of the emitter depends on neither the input fields in the future nor the output fields in the past.

# 2.2. Multi-photon scattering

Scattering of an input state into an output state is described by the (unitary) S-matrix operator  $\hat{S}$ . In particular, we consider an input state consisting of n photons  $|\mathbf{k}\rangle \equiv |k_{1,\alpha_{1}},\ldots,k_{n,\alpha_{n}}\rangle$  with frequencies  $k_{j}$  ( $j=1,\ldots,n$ ) and propagating directions  $\alpha_{j} \in \{r,l\}$ . We are interested in the composite emitter-waveguide system that conserves the total excitation number and assume that the emitter was and will be again in its ground state prior to and after the scattering. By this, the output state is also given by an n-photon state  $|\mathbf{p}\rangle \equiv |p_{1,\beta_{1}},p_{2,\beta_{2}},\ldots,p_{n,\beta_{n}}\rangle$  with generally different frequencies  $p_{j}$  satisfying the energy conservation  $\sum_{j=1}^{n} p_{j} = \sum_{j=1}^{n} k_{j}$  and different propagating directions  $\beta_{j}$ . Scattering between these input and output states is represented by the S-matrix element [25]

(2.8) 
$$S_{\mathbf{p};\mathbf{k}}^{(n)} = \langle \mathbf{p} | \hat{S} | \mathbf{k} \rangle = \langle 0 | \prod_{j=1}^{n} \hat{b}_{\beta_{j},\text{out}}(p_{j}) \prod_{j=1}^{n} \hat{b}_{\alpha_{j},\text{in}}^{\dagger}(k_{j}) | 0 \rangle,$$

where  $\hat{b}_{\alpha,\text{in}}(k)$  and  $\hat{b}_{\alpha,\text{out}}(p)$  are the input and output fields in the frequency domain, which are related to those in the time domain as

(2.9) 
$$\hat{b}_{\alpha,\text{in/out}}(k) = \frac{1}{\sqrt{2\pi}} \int dt \hat{b}_{\alpha,\text{in/out}}(t) e^{ikt}.$$

We follow Refs. [22, 44] to introduce a general scheme to compute  $S_{\mathbf{p};\mathbf{k}}^{(n)}$  for an arbitrary n. We first use Eq. (2.9) to recast  $S_{\mathbf{p};\mathbf{k}}^{(n)}$  to

(2.10) 
$$S_{\mathbf{p};\mathbf{k}}^{(n)} = F^{(n)}\langle 0| \prod_{j=1}^{n} \hat{b}_{\beta_{j},\text{out}}(t_{j}) \prod_{j=1}^{n} \hat{b}_{\alpha_{j},\text{in}}^{\dagger}(t'_{j})|0\rangle,$$

where  $F^{(n)}$  denotes a multi-dimensional Fourier transform given by

(2.11) 
$$F^{(n)} = \frac{1}{(2\pi)^n} \int \cdots \int \prod_{j=1}^n dt_j dt'_j e^{ip_j t_j - ik_j t'_j}.$$

We then use the input-output and causality relations in Eqs. (2.6) and (2.7) to represent the field correlation function in Eq. (2.10)

(2.12) 
$$\langle 0 | \prod_{i=1}^{n} \hat{b}_{\beta_{j}, \text{out}}(t_{j}) \prod_{i=1}^{n} \hat{b}_{\alpha_{j}, \text{in}}^{\dagger}(t'_{j}) | 0 \rangle,$$

in terms of the emitter correlation functions, which is the key idea in the scheme of interest. This includes the following steps:

(i) The output operators  $\hat{b}_{\beta_j,\text{out}}$  commute with each other, so that we introduce the time-ordering operator  $\mathbf{T}$  to freely order them by decreasing times. We also use Eq. (2.6) to rewrite the operator product in Eq. (2.12) as (2.13)

$$\mathbf{T}[(\hat{b}_{\beta_1,\text{in}}(t_1) + \sqrt{\gamma_{\beta_1}}\hat{c}(t_1))...(\hat{b}_{\beta_n,\text{in}}(t_n) + \sqrt{\gamma_{\beta_n}}\hat{c}(t_n))]\hat{b}_{\alpha_1,\text{in}}^{\dagger}(t_1')...\hat{b}_{\alpha_n,\text{in}}^{\dagger}(t_n').$$

We expand this product and label different terms by the number of times,  $m_t$  that the emitter operator  $\hat{c}(t_m)$  appears in each term.

(ii) Owing to the causality relation  $[\hat{c}(t), \hat{b}_{\alpha,\text{in}}(t')] = 0$  for t' > t in Eq. (2.7a), all the input operators  $\hat{b}_{\beta_j,\text{in}}$  can be moved to the right of the emitter operators  $\hat{c}$  and put outside of the time-ordering operator **T**. The  $m^{\text{th}}$ -order term in Eq. (2.13) is then

$$(2.14) \quad \langle 0|\mathbf{T}[\hat{c}(t_1)...\hat{c}(t_m)]\hat{b}_{\beta_{m+1},\text{in}}(t_{m+1})...\hat{b}_{\beta_n,\text{in}}(t_n)\hat{b}_{\alpha_1,\text{in}}^{\dagger}(t_1')...\hat{b}_{\alpha_n,\text{in}}^{\dagger}(t_n')|0\rangle\rangle.$$

(iii) We further reduce Eq. (2.14) by considering

$$\hat{b}_{\beta_{m+1},\text{in}}(t_{m+1})...\hat{b}_{\beta_n,\text{in}}(t_n)\hat{b}_{\alpha_1,\text{in}}^{\dagger}(t_1')...\hat{b}_{\alpha_n,\text{in}}^{\dagger}(t_n')|0\rangle.$$

We move  $\hat{b}_{\alpha_j,\text{in}}^{\dagger}$  to the left of  $\hat{b}_{\beta_l,\text{in}}$  using the commutation relation in Eq. (2.5a) and successively eliminate any residual  $\hat{b}_{\beta_l,\text{in}}$  in the expression. This manipulation decomposes Eq. (2.14) into in a number of terms, each in the form of a product of n-m (Dirac) delta functions and a correlation function given by

(2.15) 
$$\langle 0|\mathbf{T}[\hat{c}(t_1)...\hat{c}(t_m)]\hat{b}_{\alpha_1,\text{in}}^{\dagger}(t_1')...\hat{b}_{\text{in}}^{\dagger}(\alpha_m,t_m')|0\rangle.$$

(iv) Since  $[\hat{c}(t), \hat{b}^{\dagger}_{\alpha, \text{in}}(t')] = 0$  for t < t' following Eq. (2.7a), we can expand the time-ordering operator **T** to all the operators in Eq. (2.15). We also use the Hermitian conjugate of Eq. (2.6), i.e.,  $\hat{b}^{\dagger}_{\alpha, \text{in}}(t) = \hat{b}^{\dagger}_{\alpha, \text{out}}(t) - \sqrt{\gamma_{\alpha}} \hat{c}^{\dagger}(t)$ , to rewrite Eq. (2.15) as (2.16)

$$\langle 0|\mathbf{T}[\hat{c}(t_1)...\hat{c}(t_m)(\hat{b}_{\alpha_1,\text{out}}^{\dagger}(t_1') - \sqrt{\gamma_{\alpha_1}}\hat{c}^{\dagger}(t_1'))...(\hat{b}_{\alpha_m,\text{out}}^{\dagger}(t_m') - \sqrt{\gamma_{\alpha_m}}\hat{c}^{\dagger}(t_m'))]|0\rangle.$$

Due to the causality relation  $[\hat{c}(t), \hat{b}^{\dagger}_{\alpha_j, \text{out}}(t')] = 0$  for t > t' in Eq. (2.7b), the output operators  $\hat{b}^{\dagger}_{\alpha_j, \text{out}}$  commute with all the system operators  $\hat{c}$  to their left.

This implies that upon fully expanding Eq. (2.16) the only term that remains is

(2.17) 
$$\langle 0|\mathbf{T}[\hat{c}(t_1)...\hat{c}(t_m)\hat{c}^{\dagger}(t_1')...\hat{c}^{\dagger}(t_m')]|0\rangle.$$

After the above steps, one sees that n-photon S-matrix element  $S_{\mathbf{p};\mathbf{k}}^{(n)}$  can be computed via Fourier transform of the emitter's correlation functions

(2.18) 
$$S_{\mathbf{p};\mathbf{k}}^{(n)} = F^{(n)} \sum_{m} f_{m} \langle 0 | \mathbf{T}[\hat{c}(t_{1})...\hat{c}(t_{m})\hat{c}^{\dagger}(t_{1}')...\hat{c}^{\dagger}(t_{m}')] | 0 \rangle,$$

where each coefficient  $f_m$  contains coupling constants and delta functions.

We note that in Eq. (2.18) the emitter operators  $\hat{c}(t)$  are Heisenberg operators governed by the total emitter-waveguide Hamiltonian  $\hat{H}$ . Using the quantum regression formula [22, 43] or the Green's function technique [44], we can eliminate the waveguide degrees of freedom in the total evolution and prove that the correlation functions in Eq. (2.18) can be evaluated via an effective emitter evolution in the form

(2.19)

$$\langle 0|\mathbf{T}[\hat{c}(t_1)...\hat{c}(t_m)\hat{c}^{\dagger}(t_1')...\hat{c}^{\dagger}(t_m')]|0\rangle = \langle 0|\mathbf{T}[\hat{\tilde{c}}(t_1)...\hat{\tilde{c}}(t_m)\hat{\tilde{c}}^{\dagger}(t_1')...\hat{\tilde{c}}^{\dagger}(t_m')]|0\rangle,$$

where

$$\hat{c}(t) = e^{i\hat{H}_{\text{eff}}t}\hat{c}e^{-i\hat{H}_{\text{eff}}t}.$$

$$\hat{H}_{\text{eff}} = \hat{H}_{\text{emi}} - i \frac{\Gamma}{2} \hat{c}^{\dagger} \hat{c},$$

with  $\Gamma = \gamma_r + \gamma_l$  the total decaying rate of the emitter. Equation (2.18) is thus recast to

(2.22) 
$$S_{\mathbf{p};\mathbf{k}}^{(n)} = F^{(n)} \sum_{m} f_m \langle 0 | \mathbf{T} [\hat{\hat{c}}(t_1) ... \hat{\hat{c}}(t_m) \hat{\hat{c}}^{\dagger}(t_1') ... \hat{\hat{c}}^{\dagger}(t_m')] | 0 \rangle.$$

This is the core result that will be used repeatedly in what follows.

## 2.3. The simplest quantum emitter

So far we have kept the emitter Hamiltonian  $\hat{H}_{\rm emi}$  and its operator  $\hat{c}$  unspecified with an implication that the input-output formalism presented above is general and can be applied to various types of quantum emitters. In the following, we consider the simplest quantum emitter model, which is a two-level atom, and exemplify the above-introduced input-output technique in computing one-photon and two-photon scattering processes. Discretely, for a two-level emitter, we have

$$\hat{H}_{\rm emi} = \frac{\Omega}{2} \hat{\sigma}_z, \quad \hat{c} = \hat{\sigma}_-, \quad \hat{c}^\dagger = \hat{\sigma}_+,$$

where  $\Omega$  is the emitter transition frequency,  $\hat{\sigma}_z = |e\rangle\langle e| - |g\rangle\langle g|$ ,  $\hat{\sigma}_- = |g\rangle\langle e|$ , and  $\hat{\sigma}_+ = |e\rangle\langle g|$ . We thus also have

$$\hat{H}_{\text{eff}} = \frac{\Omega}{2}\hat{\sigma}_z - i\frac{\Gamma}{2}\hat{\sigma}_+\hat{\sigma}_-,$$

(2.25) 
$$\hat{\hat{\sigma}}_{\pm}(t) = e^{\pm (i\Omega + \frac{\Gamma}{2})t} \hat{\sigma}_{\pm},$$

$$\hat{b}_{\alpha,\text{out}}(t) = \hat{b}_{\alpha,\text{in}}(t) + \sqrt{\gamma_{\alpha}}\hat{\sigma}_{-}(t).$$

# 2.3.1. One-photon scattering

We consider one photon transmitting through the emitter, so the input and output photons co-propagate in the same direction, say,  $\alpha$ . The one-photon S-matrix element in this case is given by

(2.27) 
$$S_{p_{\alpha};k_{\alpha}}^{(1)} = \frac{1}{2\pi} \iint dt_1 dt_1' e^{i(pt_1 - kt_1')} \langle 0|\hat{b}_{\alpha,\text{out}}(t_1)\hat{b}_{\alpha,\text{in}}^{\dagger}(t_1')|0\rangle.$$

We expand the correlator  $\langle 0|\hat{b}_{\alpha,\mathrm{out}}(t_1)\hat{b}_{\alpha,\mathrm{in}}^{\dagger}(t_1')|0\rangle$  following the four steps outlined in Subsection 2.2

(2.28) 
$$\langle 0|\hat{b}_{\alpha,\text{out}}(t_1)\hat{b}_{\alpha,\text{in}}^{\dagger}(t_1')|0\rangle = \delta(t_1 - t_1') - \gamma_{\alpha}\langle 0|\mathbf{T}[\hat{\tilde{\sigma}}_{-}(t_1)\hat{\tilde{\sigma}}_{+}(t_1')]|0\rangle.$$

The first term in Eq. (2.28) contributes to  $S_{p_{\alpha};k_{\alpha}}^{(1)}$  as

$$(2.29) \delta(p-k).$$

Meanwhile, the second term in Eq. (2.28) contributes

$$(2.30) -\delta(p-k)\frac{i\gamma_{\alpha}}{d_k},$$

where

$$(2.31) d_k = k - \Omega + i\frac{\Gamma}{2}.$$

In deriving the result in Eq. (2.30) we have replaced the time-ordering operator **T** by the Heaviside function  $\Theta(t_1 - t_1')$ , and used the identity  $\int dt' e^{-i\omega t'} \Theta(t - t') = e^{-i\omega t} (i/\omega + \delta(\omega))$ . We therefore find that

(2.32) 
$$S_{p_{\alpha};k_{\alpha}}^{(1)} = \delta(p-k)t_{k},$$

where

(2.33) 
$$t_k = \frac{k - \Omega - i(\gamma_\alpha - \gamma_{\bar{\alpha}})/2}{k - \Omega + i(\gamma_\alpha + \gamma_{\bar{\alpha}})/2}.$$

with  $\bar{\alpha}$  denoting the propagating direction opposite to  $\alpha$ . The delta function in Eq. (2.32) represents the energy conservation, while  $t_k$  represents the transmission coefficient.

Setting  $\gamma_{\bar{\alpha}} = 0$  such that the (chiral) waveguide allows propagation in one direction  $\alpha$  only,  $t_k$  is reduced to

(2.34) 
$$t_k^{\text{(chiral)}} = \frac{k - \Omega - i\gamma_\alpha/2}{k - \Omega + i\gamma_\alpha/2}.$$

One sees that  $|t_k^{(\text{chiral})}| = 1$ , implying the single photon is completely transmitted through the emitter while experiencing some phase shift. Meanwhile for a non-chiral waveguide with  $\gamma_{\alpha} = \gamma_{\bar{\alpha}}$ ,  $t_k$  is of the form

(2.35) 
$$t_k^{\text{(non-chiral)}} = \frac{k - \Omega}{k - \Omega + i\Gamma/2},$$

which shows that when the single photon is on resonance with the two-level emitter  $(k = \Omega)$  its transmission through the emitter is forbidden completely or in other words the input photon is reflected completely. This complete transmission blockage is a consequence of a destructive interference between a single photon that intactly passes through the emitter and another one with a  $\pi$  phase shift that is emitted from the re-emission of the emitter after being excited to its excited state.

We consider the remaining case of one photon scattering, that is, reflection off the emitter with the input and output photons propagating in opposite directions. The S-matrix element for this reflection process is given by

(2.36) 
$$S_{p_{\bar{\alpha}};k_{\alpha}}^{(1)} = \delta(p-k)r_k,$$

where  $r_k$  is the reflection coefficient

(2.37) 
$$r_k = \frac{-i\sqrt{\gamma_{\bar{\alpha}}\gamma_{\alpha}}}{k - \Omega + i(\gamma_{\alpha} + \gamma_{\bar{\alpha}})/2}.$$

In the chiral  $(\gamma_{\bar{\alpha}} = 0)$  and non-chiral  $(\gamma_{\alpha} = \gamma_{\bar{\alpha}})$  cases, the reflection coefficient  $r_k$  is respectively given by

$$(2.38) r_k^{\text{(chiral)}} = 0,$$

(2.38) 
$$r_k^{\text{(chiral)}} = 0,$$
(2.39) 
$$r_k^{\text{(non-chiral)}} = \frac{-i\Gamma/2}{k - \Omega + i\Gamma/2}.$$

It is evident the one-photon transmission and reflection coefficients,  $t_k$  and  $r_k$ , in both chiral and non-chiral cases satisfy

$$(2.40) |t_k|^2 + |r_k|^2 = 1,$$

which reflects the conservation of one-photon scattering probability. When there is no coupling between the waveguide and the emitter, i.e.,  $\gamma_{\alpha} = \gamma_{\bar{\alpha}} = 0$ , we find  $t_k = 1$  and  $r_k = 0$ .

We can express a general one-photon scattering from an arbitrary input photon in state  $|k_{\alpha}\rangle$  into the output photon in state  $|p_{\beta}\rangle$  in terms of the S-matrix element of the form

$$(2.41) S_{p_{\beta};k_{\alpha}}^{(1)} = \delta(p-k)[\delta_{\beta,\alpha}t_k + (1-\delta_{\beta,\alpha})r_k].$$

# 2.3.2. Two-photon scattering

We consider two input photons  $|k_{1,\alpha}, k_{2,\alpha}\rangle$  co-transmitting through the emitter with the output photons  $|p_{1,\alpha}, p_{2,\alpha}\rangle$ . The S-matrix element for this two-photon scattering is given by

$$S_{p_{1,\alpha}p_{2,\alpha};k_{1,\alpha}k_{2,\alpha}}^{(2)} = \frac{1}{(2\pi)^{2}} \iiint dt_{1}dt_{2}dt'_{1}dt'_{2}e^{i(p_{1}t_{1}+p_{2}t_{2}-k_{1}t'_{1}-k_{2}t'_{2})}$$

$$(2.42) \times \langle 0|\hat{b}_{\alpha,\text{out}}(t_{1})\hat{b}_{\alpha,\text{out}}(t_{2})\hat{b}_{\alpha,\text{in}}^{\dagger}(t'_{1})\hat{b}_{\alpha,\text{in}}^{\dagger}(t'_{2})|0\rangle.$$

We follow the scheme in Subsection 2.2 to expand the correlator in Eq. (2.42)

$$\langle 0|\hat{b}_{\alpha,\text{out}}(t_{1})\hat{b}_{\alpha,\text{out}}(t_{2})\hat{b}_{\alpha,\text{in}}^{\dagger}(t_{1}')\hat{b}_{\alpha,\text{in}}^{\dagger}(t_{2}')|0\rangle$$

$$= \delta(t_{1} - t_{1}')\delta(t_{2} - t_{2}') + \delta(t_{1} - t_{2}')\delta(t_{2} - t_{1}')$$

$$-\gamma_{\alpha}\delta(t_{1} - t_{1}')\langle 0|\mathbf{T}[\hat{\sigma}_{-}(t_{2})\hat{\sigma}_{+}(t_{2}')]|0\rangle - \gamma_{\alpha}\delta(t_{1} - t_{2}')\langle 0|\mathbf{T}[\hat{\sigma}_{-}(t_{2})\hat{\sigma}_{+}(t_{1}')]|0\rangle$$

$$-\gamma_{\alpha}\delta(t_{2} - t_{1}')\langle 0|\mathbf{T}[\hat{\sigma}_{-}(t_{1})\hat{\sigma}_{+}(t_{2}')]|0\rangle - \gamma_{\alpha}\delta(t_{2} - t_{2}')\langle 0|\mathbf{T}[\hat{\sigma}_{-}(t_{1})\hat{\sigma}_{+}(t_{1}')]|0\rangle$$

$$+\gamma_{\alpha}^{2}\langle 0|\mathbf{T}[\hat{\sigma}_{-}(t_{1})\hat{\sigma}_{-}(t_{2})\hat{\sigma}_{+}(t_{1}')\hat{\sigma}_{+}(t_{2}')]|0\rangle.$$

(2.43)

The first and second terms in Eq. (2.43) contribute to  $S_{p_{1,\alpha},p_{1,\alpha};k_{1,\alpha},k_{1,\alpha}}^{(2)}$  the following

$$(2.44) \delta(p_1 - k_1)\delta(p_2 - k_2) + \delta(p_1 - k_2)\delta(p_2 - k_1).$$

The third to sixth terms in Eq. (2.43) contribute respectively

$$-\left(\delta(p_1 - k_1)\delta(p_2 - k_2) + \delta(p_1 - k_2)\delta(p_2 - k_1)\right)\frac{i\gamma_{\alpha}}{d_{p_2}}$$

$$-\left(\delta(p_2 - k_1)\delta(p_1 - k_2) + \delta(p_2 - k_2)\delta(p_1 - k_1)\right)\frac{i\gamma_{\alpha}}{d_{p_1}}.$$
(2.45)

Contribution of the last term in Eq. (2.43) to  $S_{p_{1,\alpha},p_{2,\alpha};k_{1,\alpha},k_{2,\alpha}}^{(2)}$  is more involved and given by a fourfold integral

(2.46) 
$$\frac{\gamma_{\alpha}^{2}}{(2\pi)^{2}} \iiint dt_{1}dt_{2}dt'_{1}dt'_{2}e^{i(p_{1}t_{1}+p_{2}t_{2}-k_{1}t'_{1}-k_{2}t'_{2})} \times \langle 0|\mathbf{T}[\hat{\sigma}_{-}(t_{1})\hat{\sigma}_{-}(t_{2})\hat{\sigma}_{+}(t'_{1})\hat{\sigma}_{+}(t'_{2})]|0\rangle.$$

Noting that  $\langle 0|\mathbf{T}[\hat{\hat{\sigma}}_{-}(t_1)\hat{\hat{\sigma}}_{-}(t_2)\hat{\hat{\sigma}}_{+}(t_1')\hat{\hat{\sigma}}_{+}(t_2')]|0\rangle$  is non-zero only when it starts with  $\hat{\hat{\sigma}}_{-}$  and terminates with  $\hat{\hat{\sigma}}_{+}$ , we decompose Eq. (2.46) to four integrals

$$\frac{\gamma_{\alpha}^2}{(2\pi)^2} (I_{p_1k_1p_2k_2} + I_{p_1k_2p_2k_1} + I_{p_2k_1p_1k_2} + I_{p_2k_2p_1k_1}),$$

where

$$I_{p_1k_1p_2,k_2} = \iiint dt_1 dt_2 dt'_1 dt'_2 e^{i(p_1t_1+p_2t_2-k_1t'_1-k_2t'_2)}$$

$$(2.47) \qquad \times \langle 0|\hat{\sigma}_-(t_1)\hat{\sigma}_+(t'_1)\hat{\sigma}_-(t_2)\hat{\sigma}_+(t'_2)|0\rangle\Theta(t_1-t'_1)\Theta(t'_1-t_2)\Theta(t_2-t'_2),$$

for the time ordering  $t_1 > t'_1 > t_2 > t'_2$  and similarly for  $I_{p_1k_2p_2k_1}$ ,  $I_{p_2k_1p_1k_2}$  and  $I_{p_2k_2p_1k_1}$  with the corresponding time orderings. In fact, given  $I_{p_1k_1p_2k_2}$ , the other three integrals are obtained by permuting between  $k_1$  and  $k_2$  and/or between  $p_1$  and  $p_2$ . These integrals are explicitly given by

$$\begin{split} I_{p_1k_1p_2k_2} &= -\frac{2\pi}{d_{k_2}d_{p_1}} \Big(\frac{i\delta(p_1+p_2-k_1-k_2)}{k_2-p_2} + \pi\delta(k_1-p_1)\delta(k_2-p_2)\Big), \\ I_{p_1k_2p_2k_1} &= -\frac{2\pi}{d_{k_1}d_{p_1}} \Big(\frac{i\delta(p_1+p_2-k_1-k_2)}{k_1-p_2} + \pi\delta(k_1-p_2)\delta(k_2-p_1)\Big), \\ I_{p_2k_1p_1k_2} &= -\frac{2\pi}{d_{k_2}d_{p_2}} \Big(\frac{i\delta(p_1+p_2-k_1-k_2)}{k_2-p_1} + \pi\delta(k_1-p_2)\delta(k_2-p_1)\Big), \\ I_{p_2k_2p_1k_1} &= -\frac{2\pi}{d_{k_1}d_{p_2}} \Big(\frac{i\delta(p_1+p_2-k_1-k_2)}{k_1-p_1} + \pi\delta(k_1-p_1)\delta(k_2-p_2)\Big), \end{split}$$

so the last term in Eq. (2.43) contributes to  $S^{(2)}_{p_{1,\alpha},p_{2,\alpha};k_{1,\alpha},k_{2,\alpha}}$  as

$$\frac{i\gamma_{\alpha}^{2}}{\pi} \frac{d_{p_{1}} + d_{p_{2}}}{d_{p_{1}}d_{p_{2}}d_{k_{1}}d_{k_{2}}} \delta(p_{1} + p_{2} - k_{1} - k_{2}) 
-\frac{\gamma_{\alpha}^{2}}{d_{p_{1}}d_{p_{2}}} \delta(p_{1} - k_{1})\delta(p_{2} - k_{2}) - \frac{\gamma_{\alpha}^{2}}{d_{p_{1}}d_{p_{2}}} \delta(p_{1} - k_{2})\delta(p_{2} - k_{1}).$$
(2.48)

Combining all contributions computed above yields

$$S_{p_{1,\alpha}p_{2,\alpha};k_{1,\alpha}k_{2,\alpha}}^{(2)} = S_{p_{1,\alpha};k_{1,\alpha}}^{(1)} S_{p_{2,\alpha};k_{2,\alpha}}^{(1)} + S_{p_{1,\alpha};k_{2,\alpha}}^{(1)} S_{p_{2,\alpha};k_{1,\alpha}}^{(1)} + \mathcal{B}_{p_{1,\alpha},p_{2,\alpha};k_{1,\alpha},k_{2,\alpha}}^{(2)},$$

where  $S_{p_{i,\delta};k_{l,\alpha}}^{(1)}$  is given in Eq. (2.41) and

$$(2.50) \mathcal{B}_{p_{1,\alpha},p_{2,\alpha};k_{1,\alpha},k_{2,\alpha}}^{(2)} = \frac{i\gamma_{\alpha}^2}{\pi} \frac{d_{p_1} + d_{p_2}}{d_{p_1}d_{p_2}d_{k_1}d_{k_2}} \delta(p_1 + p_2 - k_1 - k_2).$$

Equation (2.49) shows that the transmission of two photons through the emitter is composed of two types of processes. The first type is that the two photons transmit independently such as  $|k_{1,\alpha}\rangle \to |p_{1,\alpha}\rangle$  and  $|k_{2,\alpha}\rangle \to |p_{2,\alpha}\rangle$  or  $|k_{1,\alpha}\rangle \to |p_{2,\alpha}\rangle$  $|p_{2,\alpha}\rangle$  and  $|k_{2,\alpha}\rangle \to |p_{1,\alpha}\rangle$ , resulting in the first two products of one-photon S-matrix elements in Eq. (2.49). The second type is that the two photons bind with each other forming a two-photon bound state [25], which is represented by the last single expression in Eq. (2.49). Such bound state can be explained via stimulated emission in the following way. The first photon promotes the emitter to its excited state. The second photon passing through cannot be absorbed by the already excited emitter but can stimulate the emitter's re-emission of the first photon. The two photons appear together with the same phase forming a joint two-photon bound state [26]. The bound state is characterised by a common delta function  $\delta(p_1 + p_2 - k_1 - k_2)$  that indicates energy conservation for the input and output pairs as a whole, but not for independent photons. This is the origin of the so-called frequency mixing or spectral entanglement in two-photon scattering, which introduces a major challenge in constructing a controlled-phase gate for single photons from cross-Kerr nonlinearity [23, 24].

We consider more two-photon scattering scenarios in Appendix A and summarise here the most general case with arbitrary two-photon input  $|k_{1,\alpha_1}k_{2,\alpha_2}\rangle$  and output states  $|p_{1,\beta_1}p_{2,\beta_2}\rangle$ 

$$S_{p_{1,\beta_{1}},p_{2,\beta_{2}};k_{1,\alpha_{1}},k_{2,\alpha_{2}}}^{(2)} = S_{p_{1,\beta_{1}};k_{1,\alpha_{1}}}^{(1)} S_{p_{2,\beta_{2}};k_{2,\alpha_{2}}}^{(1)} + S_{p_{1,\beta_{1}};k_{2,\alpha_{2}}}^{(1)} S_{p_{2,\beta_{2}};k_{1,\alpha_{1}}}^{(1)}$$

$$+ \mathcal{B}_{p_{1,\beta_{1}},p_{2,\beta_{2}};k_{1,\alpha_{1}},k_{2,\alpha_{2}}}^{(2)},$$

where

(2.52)

$$\mathcal{B}_{p_{1,\beta_{1}},p_{\bar{2},\beta_{2}};k_{1,\alpha_{1}},k_{2,\alpha_{2}}}^{(2)} = \frac{i\sqrt{\gamma_{\beta_{1}}\gamma_{\beta_{2}}\gamma_{\alpha_{1}}\gamma_{\alpha_{2}}}}{\pi} \frac{d_{p_{1}} + d_{p_{2}}}{d_{p_{1}}d_{p_{2}}d_{k_{1}}d_{k_{2}}} \delta(p_{1} + p_{2} - k_{1} - k_{2}).$$

Similar to Eq. (2.49), Eq. (2.51) consists of products of independent one-photon scatterings as well as a two-photon bound state. This decomposition into non-bound and bound states is an essential characteristic of multi-photon scattering. In Appendix B, we show the n-photon S-matrix element  $S_{\mathbf{p};\mathbf{k}}^{(n)}$  in the form of cluster decomposition as well as a general expression for the n-photon bound state.

# 3. Scattering between a single photon and a weak coherent state

In this section, we consider scattering between a pair of input states which consists of a single photon and a weak coherent state counter-propagating to a two-level emitter embedded in a 1D waveguide, as depicted in Fig. 1. The weak coherent state can be well approximated by a superposition of vacuum and one-photon states, thus converting the scattering problem of interest into one-photon and two-photon scatterings. In practical experiments, any photon states with a finite photon number are of the form of a wavepacket [45], so we adopt a continuous-mode treatment for both the input states which are thus described by appropriate wavepackets.

# 3.1. Continuous-mode input and output states

In the continuous-mode treatment, a photon propagating in the direction  $\alpha$  is described by a wavepacket which is in turn considered as a Fock state  $|1_{F,\alpha}\rangle$  with its boson creation operator given by [45]

(3.1) 
$$\hat{b}_{F,\alpha}^{\dagger} = \int dk \psi_F(k) \hat{b}_{\alpha}^{\dagger}(k),$$

where  $\psi_F(\eta)$  is the wavepacket amplitude which due to the commutation requirement  $[\hat{b}_{F,\alpha},\hat{b}_{F,\alpha}^{\dagger}]=1$  satisfies the normalisation condition

(3.2) 
$$\int dk |\psi_F(k)|^2 = 1.$$

Using this definition, a continuous-mode n-photon Fock state propagating to the direction  $\alpha$  is given by (3.3)

$$|n_{F,\alpha}\rangle = \frac{(\hat{b}_{F,\alpha}^{\dagger})^n}{\sqrt{n!}}|0\rangle = \frac{1}{\sqrt{n!}}\int dk_1 \dots dk_n \psi_F(k_1) \dots \psi_F(k_n)|k_{1,\alpha} \dots k_{n,\alpha}\rangle.$$

A continuous-mode coherent state  $|\eta_{\alpha}\rangle$  of propagating direction  $\alpha$  is of the form [45]

(3.4) 
$$|\eta_{\alpha}\rangle = e^{-\frac{|\eta|^2}{2}} e^{\hat{b}_{\eta,\alpha}^{\dagger}} |0\rangle,$$

where  $|\eta|^2$  represents the mean photon number and  $\hat{b}_{\eta,\alpha}^{\dagger}$  is the coherent-state wavepacket creation operator with the propagating direction  $\alpha$ 

(3.5) 
$$\hat{b}_{\eta,\alpha}^{\dagger} = \int dk \psi_{\eta}(k) \hat{b}_{\alpha}^{\dagger}(k),$$

with the amplitude  $\psi_{\eta}(k)$  satisfying the normalisation condition

(3.6) 
$$\int dk |\psi_{\eta}(k)|^2 = |\eta|^2.$$

Unlike  $\hat{b}_{F,\alpha}$  and  $\hat{b}_{F,\alpha}^{\dagger}$ ,  $\hat{b}_{\eta,\alpha}$  and  $\hat{b}_{\eta,\alpha}^{\dagger}$  obey the commutation relation  $[\hat{b}_{\eta,\alpha},\hat{b}_{\eta,\alpha}^{\dagger}] = |\eta|^2$ . Since we are interested in a weak coherent state with  $|\eta|^2 \ll 1$ , we can approximate  $|\eta_{\alpha}\rangle$  as

(3.7) 
$$|\eta_{\alpha}\rangle \simeq e^{-\frac{|\eta|^2}{2}} (1 + \hat{b}_{\eta,\alpha}^{\dagger})|0\rangle = e^{-\frac{|\eta|^2}{2}}|0\rangle + e^{-\frac{|\eta|^2}{2}} \int dk \psi_{\eta}(k)|k_{\alpha}\rangle.$$

Therefore, the total input state with a single photon propagating to the right and a weak coherent state propagating to the left is

$$|\Psi_{\rm in}\rangle \equiv |1_{F,r}\rangle |\eta_l\rangle \simeq e^{-\frac{|\eta|^2}{2}} \int dk_1 \psi_F(k_1) |k_{1,r}\rangle + e^{-\frac{|\eta|^2}{2}} \iint dk_1 dk_2 \psi_F(k_1) \psi_\eta(k_2) |k_{1,r}k_{2,l}\rangle.$$
(3.8)

This input state, after propagating in the 1D waveguide and interacting with the two-level emitter, gives rise to an output state given by

$$|\Psi_{\text{out}}\rangle \equiv \hat{S}|1_{F,r}\rangle|\eta_{l}\rangle \simeq e^{-\frac{|\eta|^{2}}{2}} \int dk_{1}\psi_{F}(k_{1})\hat{S}|k_{1,r}\rangle$$

$$+e^{-\frac{|\eta|^{2}}{2}} \iint dk_{1}dk_{2}\psi_{F}(k_{1})\psi_{\eta}(k_{2})\hat{S}|k_{1,r}k_{2,l}\rangle,$$
(3.9)

where the S-matrix operator  $\hat{S}$  with its one-photon and two-photon S-matrix elements was analysed in detail in Subsection 2.3.

For numerical simulations, we choose the wave packet amplitudes  $\psi_F$  and  $\psi_\eta$  to have Gaussian profiles

(3.10) 
$$\psi_F(k) = \frac{1}{(2\pi\sigma_F^2)^{\frac{1}{4}}} \exp\left(-\frac{(k-k_{0,F})^2}{4\sigma_F^2}\right),$$

(3.11) 
$$\psi_{\eta}(k) = \frac{\eta}{(2\pi\sigma_{\eta}^{2})^{\frac{1}{4}}} \exp\left(-\frac{(k-k_{0,\eta})^{2}}{4\sigma_{\eta}^{2}}\right),$$

where  $k_{0,F}$  and  $k_{0,\eta}$  are the Fock and coherent-state central carrier frequencies and  $\sigma_F$  and  $\sigma_{\eta}$  are the corresponding bandwidths. Since interaction generally is the strongest when the input photons are in resonance with the two-level emitter, we further take  $k_{0,F} = k_{0,\eta} = \Omega$ . For non-chiral waveguides, we have  $\gamma_r \equiv \gamma_l = \gamma$ .

# 3.2. Overlap with the ideal output state

In our waveguide QED scenario (see Fig. 1), the two-level emitter is expected to provide the needed nonlinearity to emulate a cross-Kerr interaction

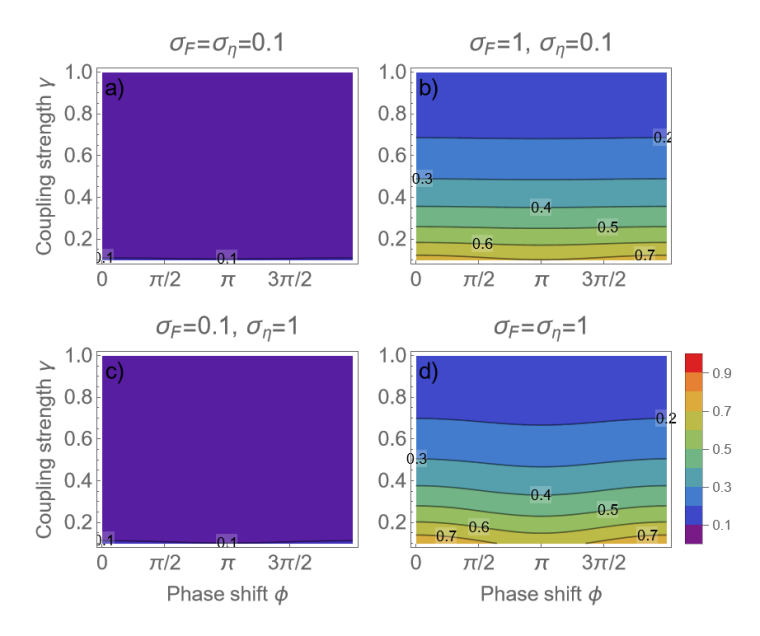


Figure 2: Overlap fidelity  $\mathcal{F}$  defined in Eq. (3.14) between the output state  $|\Psi_{\text{out}}\rangle$  and the ideal one  $|\Psi_{\text{out}}^{\text{ideal}}\rangle = |1_{F,r}\rangle|e^{i\phi}\eta_l\rangle$  as a function of the coupling strength  $\gamma$  and the phase shift  $\phi$  at  $\eta=0.2$  for a)  $\sigma_F=\sigma_\eta=0.1$ , b)  $\sigma_F=1,\sigma_\eta=0.1$ , c)  $\sigma_F=0.1,\sigma_\eta=1$ , and d)  $\sigma_F=\sigma_\eta=1$ .

between the input photon and the input coherent state in such a way that the former imparts a phase shift  $\phi$  on the latter. Concretely, the ideal output state resulting from such scattering process is given by

$$|\Psi_{\text{out}}^{\text{ideal}}\rangle \equiv |1_{F,\alpha}\rangle|e^{i\phi}\eta_{\bar{\alpha}}\rangle \simeq e^{-\frac{|\eta|^2}{2}} \int dk_1 \psi_F(k_1)|k_{1,\alpha}\rangle$$

$$+e^{-\frac{|\eta|^2}{2}} \iint dk_1 dk_2 \psi_F(k_1) \psi_{e^{i\phi}\eta}(k_2)|k_{1,\alpha}k_{2,\bar{\alpha}}\rangle,$$
(3.12)

where (as a reminder) the photon  $|1_{F,\alpha}\rangle$  and the phase-shifted coherent state  $|e^{i\phi}\eta_{\bar{\alpha}}\rangle$  should propagate in the opposite directions,  $\alpha$  and  $\bar{\alpha}$ , to be treated independently. As  $\alpha \in \{r, l\}$ , there are two possible ideal output states

(3.13) 
$$|\Psi_{\text{out}}^{\text{ideal}}\rangle \equiv \{|1_{F,r}\rangle|e^{i\phi}\eta_l\rangle, |1_{F,l}\rangle|e^{i\phi}\eta_r\rangle\}.$$

The fidelity between the output state  $|\Psi_{\rm out}\rangle$  with its the ideal counterpart  $|\Psi_{\rm out}^{\rm ideal}\rangle$  is defined as

(3.14) 
$$\mathcal{F} = |\langle \Psi_{\rm out}^{\rm ideal} | \Psi_{\rm out} \rangle|^2,$$

which following Eqs. (3.9) and (3.12) depends on the propagating direction  $\alpha$  (i.e., the explicit form of the ideal output state in Eq. (3.13)), the coupling

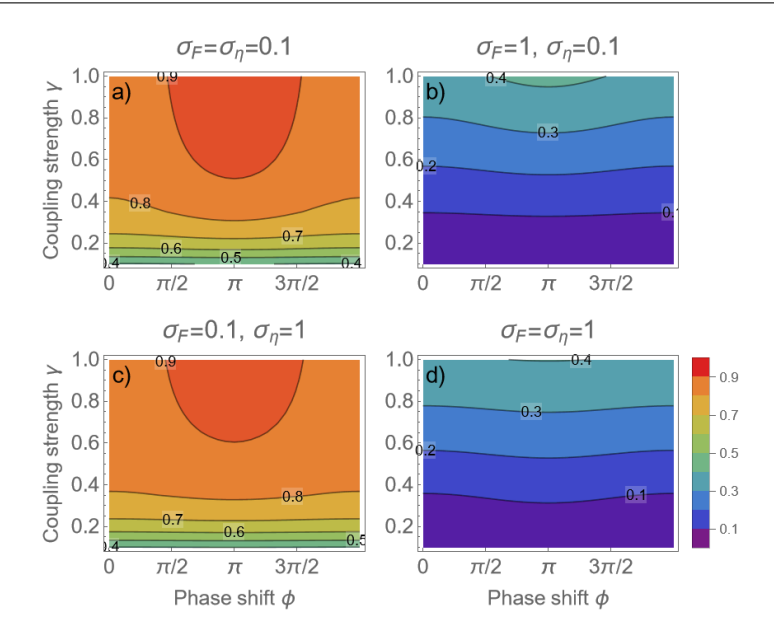


Figure 3: Overlap fidelity  $\mathcal{F}$  defined in Eq. (3.14) between the output state  $|\Psi_{\text{out}}\rangle$  and the ideal one  $|\Psi_{\text{out}}\rangle^{\text{ideal}}=|1_{F,l}\rangle|e^{i\phi}\eta_r\rangle$  as a function of the coupling strength  $\gamma$  and the phase shift  $\phi$  at  $\eta=0.2$  for a)  $\sigma_F=\sigma_\eta=0.1$ , b)  $\sigma_F=1,\sigma_\eta=0.1$ , c)  $\sigma_F=0.1,\sigma_\eta=1$ , and d)  $\sigma_F=\sigma_\eta=1$ .

strength  $\gamma$ , the phase shift  $\phi$ , the coherent-state amplitude  $\eta$ , and the two wavepacket bandwidths  $\sigma_F$  and  $\sigma_{\eta}$ , i.e.,

(3.15) 
$$\mathcal{F} \equiv \mathcal{F}(\alpha, \phi, \gamma, \eta, \sigma_F, \sigma_\eta).$$

In what follows, we fix  $\eta$  and examine how  $\mathcal{F}$  changes with  $\alpha$ ,  $\gamma$ ,  $\phi$ ,  $\sigma_F$ , and  $\sigma_n$ .

We consider  $\alpha = r$  such that  $|\Psi_{\text{out}}^{\text{ideal}}\rangle \equiv |1_{F,r}\rangle|e^{i\phi}\eta_l\rangle$ . Fixing  $\eta = 0.2$ , in Fig. 2 we plot  $\mathcal{F}$  as a function of  $\gamma$  and  $\phi$  in four bandwidth scenarios: (i)  $\sigma_F = \sigma_\eta = 0.1$ ; (ii)  $\sigma_F = 1 \gg \sigma_\eta = 0.1$ ; (iii)  $\sigma_F = 0.1 \ll \sigma_\eta = 1$ ; and (iv)  $\sigma_F = \sigma_\eta = 1$ . In all cases, we observe a common behaviour, namely, the fidelity  $\mathcal{F}$  remains essentially the same for  $\sigma_\eta = 0.1$  or  $\sigma_\eta = 1$  and depends quite weakly on the phase shift  $\phi$ . It however varies significantly when changing the Fock bandwidth  $\sigma_F$  from 0.1 to 1. In particular, for  $\sigma_F = 0.1$  (Figs. 2a and 2c)  $\mathcal{F}$  is small, < 0.1 for the whole parameter region. Meanwhile, for  $\sigma_F = 1$  (Figs. 2b and 2d)  $\mathcal{F}$  gradually reduces from above 0.7 to below 0.2 when varying  $\gamma$  from 0.1 to 1.

We repeat above analysis for  $\alpha = l$  and the ideal output state  $|\Psi_{\text{out}}^{\text{ideal}}\rangle \equiv |1_{F,l}\rangle|e^{i\phi}\eta_r\rangle$  in Fig. 3. For  $\sigma_F = 0.1$  (Figs. 3a and 3c),  $\mathcal F$  increases from 0.4 to

above 0.8 at  $\gamma \sim 0.4$  and remains > 0.8 for  $\gamma > 0.4$ . For  $\sigma_F = 1$  (Figs. 3b and 3d),  $\mathcal{F}$  improves steadily from below 0.1 to 0.4 with increasing  $\gamma$ . Comparing between Figs. 2 and 3, we see that the output state  $|\Psi_{\text{out}}\rangle$  in Eq. (3.9) is closer to  $|1_{F,r}\rangle|e^{i\phi}\eta_l\rangle$  than to  $|1_{F,l}\rangle|e^{i\phi}\eta_r\rangle$  when  $\sigma_F = 1$  and  $\gamma \sim 0.1$ . In contrast, it is closer to  $|1_{F,l}\rangle|e^{i\phi}\eta_r\rangle$  than to  $|1_{F,r}\rangle|e^{i\phi}\eta_l\rangle$  when  $\sigma_F = 0.1$  and  $\gamma \sim 1$ .

# 3.3. Photon statistics of the output state

We analyse the photon distribution of the output state in Eq. (3.9), which includes the following cases:

- One photon going to the right with a probability denoted by  $P_r^{(1)}$ ;
- One photon going to the left with a probability denoted by  $P_l^{(1)}$ ;
- Two photons going to the right with a probability denoted by  $P_{rr}^{(2)}$ ;
- Two photons going to the left with a probability denoted by  $P_{ll}^{(2)}$ ;
- One photon going to the right and one photon going to the left with a probability denoted by  $P_{rl}^{(2)}$ .

These probabilities are given by

$$(3.16) P_{\alpha}^{(1)} = \int dp_1 |\langle p_{1,\alpha} | \text{out} \rangle|^2,$$

(3.17) 
$$P_{\alpha\beta}^{(2)} = N_{\alpha\beta} \int \int dp_1 dp_2 |\langle p_{1,\alpha} p_{2,\beta} | \text{out} \rangle|^2,$$

where  $\alpha, \beta \in \{r, l\}$  and  $N_{\alpha\beta} = 1/(1 + \delta_{\alpha\beta})$ . The prefactor  $N_{\alpha\beta}$  accounts for the fact that when two photons co-propagate they are indistinguishable. Since these include all the allowed scattering processes, we have conservation of the probability

(3.18) 
$$P_r^{(1)} + P_l^{(1)} + P_{rr}^{(2)} + P_{ll}^{(2)} + P_{rl}^{(2)} = 1.$$

Using the expression of the output state  $|\Psi_{\rm out}\rangle$  in Eq. (3.9), we express the above probabilities in more explicit forms as

$$(3.19) P_{\alpha}^{(1)} = e^{-|\eta|^2} \int dp_1 dk_1' dk_1 \psi_F^*(k_1') \psi_F(k_1) \left(S_{p_{1,\alpha};k_{1,\alpha}'}^{(1)}\right)^* S_{p_{1,\alpha};k_{1,\alpha}}^{(1)},$$

with the general one-photon S-matrix element  $S_{p_{\beta};k_{0}}^{(1)}$  given in Eq. (2.41), and

$$P_{\alpha\beta}^{(2)} = N_{\alpha\beta}e^{-|\eta|^2} \int dp_1 dp_2 dk_1' dk_2' dk_1 dk_2 \psi_F^*(k_1') \psi_\eta^*(k_2') \psi_F(k_1) \psi_\eta(k_2)$$

$$(3.20) \times \left(S_{p_{1,\alpha}p_{2,\beta};k_{1,\alpha}k_{2,\beta}'}^{(2)}\right)^* S_{p_{1,\alpha}p_{2,\beta};k_{1,\alpha}k_{2,\beta}}^{(2)},$$

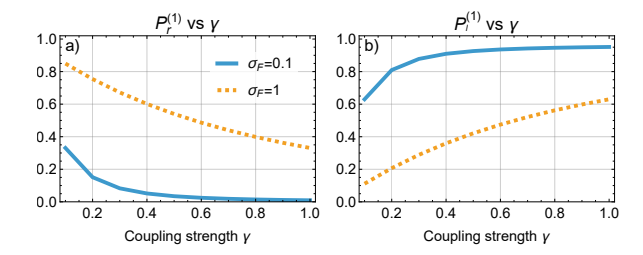


Figure 4: a) Probability  $P_r^{(1)}$  as a function of the coupling strength  $\gamma$  fixing the Fock-state bandwidth  $\sigma_F$  at 0.1 and 1. b) Same as panel a) but for  $P_l^{(1)}$ . In both panels, the input coherent-state amplitude is set to  $\eta = 0.2$ .

with the general two-photon S-matrix element  $S_{p_{1,\beta_{1}}p_{2,\beta_{2}};k_{1,\alpha_{1}}k_{2,\alpha_{2}}}^{(2)}$  given in Eq. (2.51).

Examining  $P_{\alpha}^{(1)}$  in Eq. (3.19) as well as the output state  $|\Psi_{\text{out}}\rangle$  in Eq. (3.9), one observes that one-photon scattering takes place primarily due the input single photon, while the presence of the input coherent state merely introduces a re-normalising factor  $e^{-|\eta|^2}$ . In contrast, two-photon scattering shown in  $P_{\alpha\beta}^{(2)}$  in Eq. (3.20) involves significantly both the input single photon and the input coherent state.

In Fig. 4, we plot the one-photon scattering probabilities  $P_r^{(1)}$  and  $P_l^{(1)}$  as functions of the coupling strength  $\gamma$ , fixing the input coherent-state amplitude at  $\eta = 0.2$ . Since these probabilities only depend on the wavepacket profile  $\psi_F$  of the input single photon (see Eq. (3.19)), we consider two values of the bandwidth  $\sigma_F \in \{0.1, 1\}$ . We also note that we are interested in the case  $\gamma > 0$ , so we vary  $\gamma$  from 0.1 to 1. The limit  $\gamma \to 0$  is trivial with  $P_r^{(1)} \sim 1$ (transmission) and  $P_l^{(1)} \sim 0$  (reflection) as pointed out in the zero-coupling analysis for one-photon scattering below Eq. (2.40). When  $\sigma_F = 0.1, P_r^{(1)}$  in Fig. 4a decreases from close to 0.4 to near 0 as increasing the coupling strength  $\gamma$  from 0.1 to 1, while  $P_l^{(1)}$  in Fig. 4b increases from above 0.6 to near 1. This shows that the input single photon with a narrow-band wavepacket is dominantly reflected, consistent with our analysis of  $t_k$  in Eq. (2.33). When  $\sigma_F = 1$ ,  $P_r^{(1)}$  also sees a decreasing trend as with  $\sigma_F = 0.1$ , from near 0.9 to close to 0.4.  $P_l^{(1)}$  in contrast is improved from a low value near 0.1 to over 0.6. Thus, given a broad-band wavepacket and a reasonably large coupling strength  $\gamma \sim 0.6$ , the input single photon can be equally transmitted and reflected. Both  $P_r^{(1)}$  and  $P_l^{(1)}$  see the effect of the input coherent state via a normalising factor  $e^{-|\eta|^2}\sim 0.96$  for  $\eta=0.2$ .

In Fig. 5, we plot the two-photon scattering probabilities  $P_{rr}^{(2)}$ ,  $P_{ll}^{(2)}$ , and  $P_{rl}^{(2)}$  as functions of the coupling strength  $\gamma$ , with the coherent-state amplitude

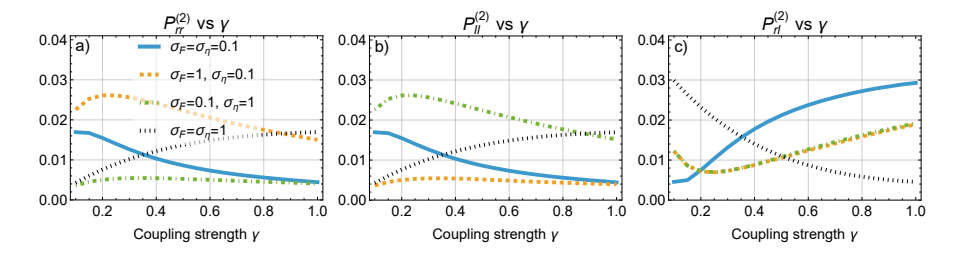


Figure 5: a) Probability  $P_{rr}^{(2)}$  as a function of the coupling strength  $\gamma$  for three cases:  $\sigma_F = \sigma_\eta = 0.1$ ;  $\sigma_F = 1$ ,  $\sigma_\eta = 0.1$ ;  $\sigma_F = 0.1$ ,  $\sigma_\eta = 0.1$ ; and  $\sigma_F = \sigma_\eta = 1$ . b) and c) Same as panel a) but for  $P_{ll}^{(2)}$  and  $P_{rl}^{(2)}$ .

 $\eta$  chosen at 0.2. Following Eq. (3.20), these probabilities depend on the photon wavepackets,  $\psi_F$  and  $\psi_\eta$ , of both the input single photon and the input coherent state so that we consider four different scenarios for the bandwidths: (i)  $\sigma_F =$  $\sigma_{\eta}=0.1$ ; (ii)  $\sigma_{F}=1\gg\sigma_{\eta}=0.1$ ; (iii)  $\sigma_{F}=0.1\ll\sigma_{\eta}=1$ ; and (iv)  $\sigma_{F}=\sigma_{\eta}=1$ . For scenario (i), where the two input states have the same narrow bandwidth, due to symmetry  $P_{rr}^{(2)}$  in Fig. 5a and  $P_{ll}^{(2)}$  in Fig. 5b are identical, gradually declining from near 0.02 to 0.005 as increasing the coupling strength  $\gamma$ . Meanwhile,  $P_{rl}^{(2)}$  in Fig. 5c increases from 0.005 to near 0.03. This indicates that in the limit of narrow bandwidths for both the input states, it is more likely to find output photons counter-propagating than co-propagating, as increasing  $\gamma$ . For scenario (ii), where the input single photon has a much larger bandwidth than that of the input coherent state,  $P_{rr}^{(2)}$  goes up to an optimal value  $\sim 0.025$  at  $\gamma \sim 0.2$ , then decreasing to near 0.015.  $P_{II}^{(2)}$  sees the same trend but its values remain below 0.005 for the whole range of  $\gamma$ . These variations in  $P_{rr}^{(2)}$  and  $P_{ll}^{(2)}$  are exactly exchanged to each other in scenario (iii).  $P_{rl}^{(2)}$  interestingly behaves the same in scenario (ii) or (iii), which decreases to a minimum at  $\gamma \sim 0.02$  and after that steadily grows to 0.02. For scenario (iv),  $P_{rr}^{(2)}$  and  $P_{II}^{(2)}$  behave the same due to symmetry increasing from just below 0.005 to near 0.02, while  $P_{rl}^{(2)}$  steadily decreases from just above 0.03 to near 0.005. Therefore, when there is a substantial difference in the input wavepacket bandwidths (i.e., scenarios (ii) and (iii)), the scattering process becomes more involved, which in general requires taking into account all the relevant scattering terms.

We confirm numerically that all the probabilities in Fig. 4 and Fig. 5 sum up to 1, thus confirming the probability conservation in Eq. (3.18). Additionally,  $P_{rr}^{(2)}$ ,  $P_{ll}^{(2)}$ , and  $P_{rl}^{(2)}$  are a small fraction compared to  $P_r^{(1)}$  or  $P_l^{(1)}$ . This agrees with our weak-coherent-state assumption, that renders one-photon terms the dominant scattering process.

#### 4. Conclusions

We have detailed an analysis of the interaction between a single photon and a weak coherent state in a waveguide QED setting: the two photon states counter-propagate along a 1D waveguide that is coupled to a two-level quantum emitter. The relevant scatterings in this setting are of one- and two-photon types, which we compute exactly using a generalised input-output framework. We have numerically analysed how close the output state is to the ideal phase-shifted output state and its photon distribution, taking into account the realistic continuous-mode wavepackets of the involved states.

This work represents a basis for tackling more challenging problems in future. For example, a weak coherent state can be replaced with an arbitrarily strong one [32] and/or a single photon replaced by an n-photon state (n > 1), which will require increasingly complex scattering analyses involving more than two photons but hold promise for intriguingly nontrivial effects such as high-fidelity large phase shift. Another consideration is to harness a three-level emitter of either ladder or lambda type [46]. This expands the possible scattering scenarios, such as two input photon states having two different polarisations allowed by the possibly different transitions of the three-level emitter and co-propagating in a 1D waveguide. In addition, application of a different input-output approach like the path integral technique [41] is of particular interest, that could potentially simplify complicated scattering calculations with large photon numbers.

#### Appendix A. More on two-photon scatterings

We list below all the relevant two-photon scattering processes in a non-chiral waveguide.

- (i) Two co-propagating input photons  $|k_{1,\alpha}, k_{2,\alpha}\rangle$ :
  - (i-1) both transmitting, with two output photons  $|p_{1,\alpha}, p_{2,\alpha}\rangle$ ;
  - (i-2) one transmitting and one reflecting, with two output photons  $|p_{1,\bar{\alpha}},p_{2,\alpha}\rangle;$
  - (i-3) both reflecting, with two output photons  $|p_{1,\bar{\alpha}}, p_{2,\bar{\alpha}}\rangle$ .
- (ii) Two counter-propagating input photons  $|k_{1,\alpha}, k_{2,\bar{\alpha}}\rangle$ :

- (ii-1) both transmitting, with two output photons  $|p_{1,\alpha}, p_{2,\bar{\alpha}}\rangle$ ;
- (ii-2) one transmitting and one reflecting, with two output photons  $|p_{1,\alpha},p_{2,\alpha}\rangle$ ;
- (ii-3) both reflecting, with two output photons  $|p_{1,\bar{\alpha}},p_{2,\alpha}\rangle$ .

The scenario (i-1) was consider in the main text. In what follows, we address the scattering scenarios (i-3) and (ii-1) with the remaining cases computed similarly. The general S-matrix element that takes into account all the scatterings above is shown in Eq. (2.51).

## A.1. Reflection of two co-propagating photons

We consider two single photons  $|k_{1,\alpha}, k_{2,\alpha}\rangle$  co-propagating to the emitter and co-reflecting through with the output photons given by  $|p_{1,\bar{\alpha}}, p_{2,\bar{\alpha}}\rangle$ . The S-matrix element for this two-photon scattering is given by

$$S_{p_{1,\bar{\alpha}}p_{2,\bar{\alpha}};k_{1,\alpha}k_{2,\alpha}}^{(2)} = \frac{1}{(2\pi)^{2}} \iiint dt_{1}dt_{2}dt'_{1}dt'_{2}e^{i(p_{1}t_{1}+p_{2}t_{2}-k_{1}t'_{1}-k_{2}t'_{2})} \times \langle 0|\hat{b}_{\bar{\alpha},\text{out}}(t_{1})\hat{b}_{\bar{\alpha},\text{out}}(t_{2})\hat{b}_{\alpha,\text{in}}^{\dagger}(t'_{1})\hat{b}_{\alpha,\text{in}}^{\dagger}(t'_{2})|0\rangle.$$

We expand the correlator in (A.1) by using the input-output relation

$$\langle 0|\hat{b}_{\bar{\alpha},\text{out}}(t_1)\hat{b}_{\bar{\alpha},\text{out}}(t_2)\hat{b}_{\alpha,\text{in}}^{\dagger}(t_1')\hat{b}_{\alpha,\text{in}}^{\dagger}(t_2')|0\rangle$$
(A.2) 
$$= \gamma_{\bar{\alpha}}\langle 0|\mathbf{T}[\hat{\sigma}_{-}(t_1)\hat{\sigma}_{-}(t_2)\hat{\sigma}_{+}(t_1')\hat{\sigma}_{+}(t_2')]|0\rangle.$$

To compute  $S^{(2)}_{p_{1,\bar{\alpha}}p_{2,\bar{\alpha}};k_{1,\alpha}k_{2,\alpha}}$ , we repeat the computation of Eq. (2.46) (just with a different prefactor now) and find that

$$(A.3) \quad \begin{aligned} S_{p_{1,\bar{\alpha}}p_{2,\bar{\alpha}};k_{1,\alpha}k_{2,\alpha}}^{(2)} \\ &= \frac{i\gamma_{\bar{\alpha}}\gamma_{\alpha}}{\pi} \frac{d_{p_{1}} + d_{p_{2}}}{d_{p_{1}}d_{p_{2}}d_{k_{1}}d_{k_{2}}} \delta(p_{1} + p_{2} - k_{1} - k_{2}) \\ &- \frac{\gamma_{\bar{\alpha}}\gamma_{\alpha}}{d_{p_{1}}d_{p_{2}}} \delta(p_{1} - k_{1})\delta(p_{2} - k_{2}) - \frac{\gamma_{\bar{\alpha}}\gamma_{\alpha}}{d_{p_{1}}d_{p_{2}}} \delta(p_{1} - k_{2})\delta(p_{2} - k_{1}) \\ &= S_{p_{1,\bar{\alpha}};k_{1,\alpha}}^{(1)} S_{p_{2,\bar{\alpha}};k_{2,\alpha}}^{(1)} + S_{p_{1,\bar{\alpha}};k_{2,\alpha}}^{(1)} S_{p_{2,\bar{\alpha}};k_{1,\alpha}}^{(1)} + \mathcal{B}_{p_{1,\bar{\alpha}},p_{2,\bar{\alpha}};k_{1,\alpha},k_{2,\alpha}}^{(2)}, \end{aligned}$$

where

(A.4) 
$$\mathcal{B}_{p_{1,\bar{\alpha}},p_{2,\bar{\alpha}};k_{1,\alpha},k_{2,\alpha}}^{(2)} = \frac{i\gamma_{\bar{\alpha}}\gamma_{\alpha}}{\pi} \frac{d_{p_{1}} + d_{p_{2}}}{d_{p_{1}}d_{p_{2}}d_{k_{1}}d_{k_{2}}} \delta(p_{1} + p_{2} - k_{1} - k_{2}).$$

# A.2. Transmission of two counter-propagating photons

We consider two photons  $|k_{1,\alpha}, k_{2,\bar{\alpha}}\rangle$  counter-propagating to the emitter and passing through each other with the output photons given by  $|p_{1,\alpha}, p_{2,\bar{\alpha}}\rangle$ . The S-matrix element for this two-photon scattering is given by

$$S_{p_{\alpha,1}p_{2,\bar{\alpha}};k_{1,\alpha}k_{2,\bar{\alpha}}}^{(2)} = \frac{1}{(2\pi)^2} \iiint dt_1 dt_2 dt'_1 dt'_2 e^{i(p_1t_1 + p_2t_2 - k_1t'_1 - k_2t'_2)}$$

$$(A.5) \qquad \times \langle 0|\hat{b}_{\alpha,\text{out}}(t_1)\hat{b}_{\bar{\alpha},\text{out}}(t_2)\hat{b}_{\alpha,\text{in}}^{\dagger}(t'_1)\hat{b}_{\bar{\alpha},\text{in}}^{\dagger}(t'_2)|0\rangle.$$

We expand the correlator in (A.5)

$$\langle 0|\hat{b}_{\alpha,\text{out}}(t_{1})\hat{b}_{\bar{\alpha},\text{out}}(t_{2})\hat{b}_{\alpha,\text{in}}^{\dagger}(t_{1}')\hat{b}_{\bar{\alpha},\text{in}}^{\dagger}(t_{2}')|0\rangle$$

$$= \delta(t_{1} - t_{1}')\delta(t_{2} - t_{2}')$$

$$-\gamma_{\bar{\alpha}}\delta(t_{1} - t_{1}')\langle 0|\mathbf{T}[\hat{\sigma}_{-}(t_{2})\hat{\sigma}_{+}(t_{2}')]|0\rangle$$

$$-\gamma_{\alpha}\delta(t_{2} - t_{2}')\langle 0|\mathbf{T}[\hat{\sigma}_{-}(t_{1})\hat{\sigma}_{+}(t_{1}')]|0\rangle$$

$$+\sqrt{\gamma_{\bar{\alpha}}}\gamma_{\alpha}\langle 0|\mathbf{T}[\hat{\sigma}_{-}(t_{1})\hat{\sigma}_{-}(t_{2})\hat{\sigma}_{+}(t_{1}')\hat{\sigma}_{+}(t_{2}')]|0\rangle.$$
(A.6)

Evaluating these terms and taking their Fourier transforms, we obtain

$$S_{p_{1,\alpha},p_{2,\bar{\alpha}};k_{1,\alpha},k_{2,\bar{\alpha}}}^{(2)} = \left(1 - \frac{i\gamma_{\alpha}}{d_{p_{1}}}\right) \left(1 - \frac{i\gamma_{\bar{\alpha}}}{d_{p_{2}}}\right) \delta(p_{1} - k_{1}) \delta(p_{2} - k_{2}) - \frac{\gamma_{\bar{\alpha}}\gamma_{\alpha}}{d_{p_{1}}d_{p_{2}}} \delta(p_{1} - k_{2}) \delta(p_{2} - k_{1})$$

$$+ \frac{i\gamma_{\bar{\alpha}}\gamma_{\alpha}}{\pi} \frac{d_{p_{1}} + d_{p_{2}}}{d_{p_{1}}d_{p_{2}}d_{k_{1}}d_{k_{2}}} \delta(p_{1} + p_{2} - k_{1} - k_{2})$$

$$= S_{p_{1,\alpha};k_{1,\alpha}}^{(1)} S_{p_{2,\bar{\alpha}};k_{2,\bar{\alpha}}}^{(1)} + S_{p_{\alpha,1};k_{2,\bar{\alpha}}}^{(1)} S_{p_{2,\bar{\alpha}};k_{1,\alpha}}^{(1)} + \mathcal{B}_{p_{1,\alpha},p_{2,\bar{\alpha}};k_{1,\alpha},k_{2,\bar{\alpha}}}^{(2)},$$

$$(A.7)$$

where

(A.8) 
$$\mathcal{B}_{p_{1,\alpha},p_{2,\bar{\alpha}};k_{1,\alpha},k_{2,\bar{\alpha}}}^{(2)} = \frac{i\gamma_{\bar{\alpha}}\gamma_{\alpha}}{\pi} \frac{d_{p_1} + d_{p_2}}{d_{p_1}d_{p_2}d_{k_1}d_{k_2}} \delta(p_1 + p_2 - k_1 - k_2).$$

## Appendix B. Cluster decomposition of multi-photon scattering

In general,  $S_{\mathbf{p};\mathbf{k}}^{(n)}$  is decomposed into non-bound or bound scattering clusters which correspond to photons propagating through the scattering region independently or forming many-body bound states, respectively [26, 44]. We

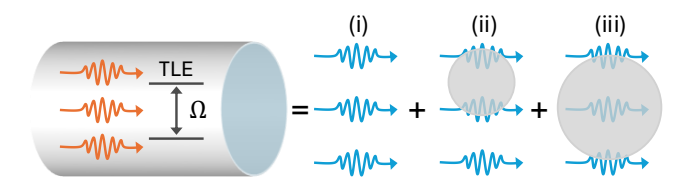


Figure 6: Cluster decomposition of n-photon scattering for n=3. Given three input photons (orange on the left) interacting with a two-level emitter in a 1D waveguide, the scattering yields three types of output photons (blue on the right): (i) three independent photons, (ii) two photons bound to each other and one independent photon, and (iii) all three photons bound to each other. The photon bound states are represented by wavepackets partially masked by a gray disk.

illustrate the general structure of *n*-photon scattering for n=3 in Fig. 6. Explicitly, this cluster decomposition of  $S_{\mathbf{p};\mathbf{k}}^{(n)}$  is formulated as [44]

(B.1) 
$$S_{\mathbf{p},\mathbf{k}}^{(n)} = \sum_{\mathcal{Q}} \sum_{P} \prod_{j=1}^{|\mathcal{Q}|} \mathcal{B}_{\mathbf{p}_{\mathcal{Q}_j};\mathbf{k}_{\mathcal{Q}P_j}}^{(|\mathcal{Q}_j|)},$$

where Q is a partition of the list  $\{1, 2, ..., n\}$  into smaller subsets  $Q_j$  with the number of subsets given by Q's cardinality |Q|, P is a permutation over the same list, QP is the same partition as Q but on the permutated list  $\{P(1), P(2), ..., P(n)\}$  with its corresponding subsets denoted by  $QP_j$ . The sum in Eq. (B.1) takes into account all the distinct permutations under the boson exchange symmetries in each partition. For example, considering n=4, a possible partition is  $Q=\{\{1,3\},\{2\},\{4\}\}\}$  with |Q|=3 and  $Q_1=\{1,3\}$ ,  $Q_2=\{2\}$ , and  $Q_3=\{4\}$ . Given a permutation  $P=\{4,2,1,3\}$  we have  $QP\equiv\{QP_j\}=\{\{4,1\},\{2\},\{3\}\}$ . Another permutation  $P'=\{1,2,4,3\}$  would lead to  $QP'\equiv\{QP'_j\}=\{\{1,4\},\{2\},\{3\}\}$ , which is the same as QP and so will not be counted in the summation.

In Eq. (B.1),  $\mathcal{B}_{\mathbf{p}_{\mathcal{Q}_{j}};\mathbf{k}_{\mathcal{Q}P_{j}}}^{(|\mathcal{Q}_{j}|)}$  represents a multi-photon bound state when  $|\mathcal{Q}_{j}| > 1$ , but is reduced to an independent one-photon scattering (i.e.,  $S_{p;k}^{(1)}$ ) when  $|\mathcal{Q}_{j}| = 1$ . The explicit expression for  $\mathcal{B}_{\mathbf{p};k}^{(n)}$ , given an n-photon input state  $|\mathbf{k}\rangle \equiv |k_{1,\alpha_{1}}, \ldots, k_{n,\alpha_{n}}\rangle$  and an n-photon state  $|\mathbf{p}\rangle \equiv |p_{1,\beta_{1}}, p_{2,\beta_{2}}, \ldots, p_{n,\beta_{n}}\rangle$ , in the case of a two-level emitter is [22]

$$\mathcal{B}_{\mathbf{p};\mathbf{k}}^{(n)} = -\frac{i}{(2\pi)^{n-1}} \prod_{j=1}^{n} (\gamma_{\alpha_j} \gamma_{\beta_j})^{\frac{1}{2}}$$
(B.2) 
$$\times \left\{ \prod_{l=1}^{n} \left( \sum_{j=1}^{l} \Delta_j \right)^{-1} \prod_{m=1}^{n} \left( k_m - \epsilon + \sum_{j=1}^{m-1} \Delta_j \right)^{-1} + \text{perms} \right\} \delta \left( \sum_{j=1}^{n} \Delta_j \right),$$

where  $\epsilon = \Omega - i\Gamma/2$  (with  $\Omega$  the emitter transition frequency and  $\Gamma = \gamma_r + \gamma_l$  the emitter total decay rate),  $\Delta_j = k_j - p_j$ , and "perms" denotes permutations taken among the input frequencies  $\{k_j\}$  and output ones  $\{p_j\}$ .

#### References

- [1] Kok, Pieter, Munro, W. J., Nemoto, Kae, Ralph, T. C., Dowling, Jonathan P., and Milburn, G. J. Linear optical quantum computing with photonic qubits. Rev. Mod. Phys., 79:135–174, Jan 2007.
- [2] Nielsen, Michael A and Chuang, Isaac L. Quantum computation and quantum information. Cambridge university press, 2010.
- [3] Knill, E., Laflamme, R., and Milburn, G. J. A scheme for efficient quantum computation with linear optics. Nature, 409(6816):46–52, 2001.
- [4] Briegel, H. J., Browne, D. E., Dür, W., Raussendorf, R., and Van den Nest, M. Measurement-based quantum computation. Nature Physics, 5(1):19–26, 2009.
- [5] Lukin, M. D. Colloquium: Trapping and manipulating photon states in atomic ensembles. Rev. Mod. Phys., 75:457–472, Apr 2003.
- [6] Lodahl, Peter, Mahmoodian, Sahand, and Stobbe, Søren. Interfacing single photons and single quantum dots with photonic nanostructures. Rev. Mod. Phys., 87:347–400, May 2015.
- [7] Vetsch, E., Reitz, D., Sagué, G., Schmidt, R., Dawkins, S. T., and Rauschenbeutel, A. Optical Interface Created by Laser-Cooled Atoms Trapped in the Evanescent Field Surrounding an Optical Nanofiber. Phys. Rev. Lett., 104:203603, May 2010.
- [8] Corzo, Neil V., Gouraud, Baptiste, Chandra, Aveek, Goban, Akihisa, Sheremet, Alexandra S., Kupriyanov, Dmitriy V., and Laurat, Julien. Large Bragg Reflection from One-Dimensional Chains of Trapped Atoms Near a Nanoscale Waveguide. Phys. Rev. Lett., 117:133603, Sep 2016.

- [9] Lund-Hansen, T., Stobbe, S., Julsgaard, B., Thyrrestrup, H., Sünner, T., Kamp, M., Forchel, A., and Lodahl, P. Experimental Realization of Highly Efficient Broadband Coupling of Single Quantum Dots to a Photonic Crystal Waveguide. Phys. Rev. Lett., 101:113903, Sep 2008.
- [10] Arcari, M., Söllner, I., Javadi, A. and Lindskov Hansen, S., Mahmoodian, S., Liu, J., Thyrrestrup, H., Lee, E. H., Song, J. D., Stobbe, S., and Lodahl, P. Near-Unity Coupling Efficiency of a Quantum Emitter to a Photonic Crystal Waveguide. Phys. Rev. Lett., 113:093603, Aug 2014.
- [11] O. Astafiev , A. M. Zagoskin , A. A. Abdumalikov , Yu. A. Pashkin , T. Yamamoto , K. Inomata , Y. Nakamura , and J. S. Tsai. Resonance Fluorescence of a Single Artificial Atom. Science, 327(5967):840–843, 2010.
- [12] Arjan F. van Loo , Arkady Fedorov , Kevin Lalumière , Barry C. Sanders , Alexandre Blais , and Andreas Wallraff. Photon-Mediated Interactions Between Distant Artificial Atoms. Science, 342(6165):1494–1496, 2013.
- [13] Sheremet, Alexandra S., Petrov, Mihail I., Iorsh, Ivan V., Poshakinskiy, Alexander V., and Poddubny, Alexander N. Waveguide quantum electrodynamics: Collective radiance and photon-photon correlations. Rev. Mod. Phys., 95:015002, Mar 2023.
- [14] Roy, Dibyendu, Wilson, C. M., and Firstenberg, Ofer. Colloquium: Strongly interacting photons in one-dimensional continuum. Rev. Mod. Phys., 89:021001, May 2017.
- [15] Chang, Darrick E., Sørensen, Anders S., Demler, Eugene A., and Lukin, Mikhail D. A single-photon transistor using nanoscale surface plasmons. Nature Physics, 3(11):807–812, 2007.
- [16] Abdumalikov, A. A., Astafiev, O., Zagoskin, A. M., Pashkin, Yu. A., Nakamura, Y., and Tsai, J. S. Electromagnetically Induced Transparency on a Single Artificial Atom. Phys. Rev. Lett., 104:193601, May 2010.
- [17] Peyronel, Thibault, Firstenberg, Ofer, Liang, Qi-Yu, Hofferberth, Sebastian, Gorshkov, Alexey V., Pohl, Thomas, Lukin, Mikhail D., and Vuletić, Vladan. Quantum nonlinear optics with single photons enabled by strongly interacting atoms. Nature, 488(7409):57–60, 2012.

- [18] Firstenberg, Ofer, Peyronel, Thibault, Liang, Qi-Yu, Gorshkov, Alexey V., Lukin, Mikhail D., and Vuletić, Vladan. Attractive photons in a quantum nonlinear medium. Nature, 502(7469):71-75, 2013.
- [19] J. T. Shen and Shanhui Fan. Coherent photon transport from spontaneous emission in one-dimensional waveguides. Opt. Lett., 30(15):2001–2003, Aug 2005.
- [20] Shen, Jung-Tsung and Fan, Shanhui. Strongly Correlated Two-Photon Transport in a One-Dimensional Waveguide Coupled to a Two-Level System. Phys. Rev. Lett., 98:153003, Apr 2007.
- [21] Shen, Jung-Tsung and Fan, Shanhui. Strongly correlated multiparticle transport in one dimension through a quantum impurity. Phys. Rev. A, 76:062709, Dec 2007.
- [22] Tommaso Caneva, Marco T Manzoni, Tao Shi, James S Douglas, J Ignacio Cirac, and Darrick E Chang. Quantum dynamics of propagating photons with strong interactions: a generalized input-output formalism. New Journal of Physics, 17(11):113001, Oct 2015.
- [23] Brod, Daniel J., Combes, Joshua, and Gea-Banacloche, Julio. Two photons co- and counterpropagating through N cross-Kerr sites. Phys. Rev. A, 94:023833, Aug 2016.
- [24] **Brod, Daniel J.** and **Combes, Joshua**. Passive CPHASE Gate via Cross-Kerr Nonlinearities. Phys. Rev. Lett., 117:080502, Aug 2016.
- [25] Fan, Shanhui , Kocabaş, Şükrü Ekin , and Shen, Jung-Tsung. Input-output formalism for few-photon transport in one-dimensional nanophotonic waveguides coupled to a qubit. Phys. Rev. A, 82:063821, Dec 2010.
- [26] Zheng, Huaixiu, Gauthier, Daniel J., and Baranger, Harold U. Waveguide QED: Many-body bound-state effects in coherent and Fock-state scattering from a two-level system. Phys. Rev. A, 82:063816, Dec 2010.
- [27] Nemoto, Kae and Munro, W. J. Nearly Deterministic Linear Optical Controlled-NOT Gate. Phys. Rev. Lett., 93:250502, Dec 2004.
- [28] T P Spiller, Kae Nemoto, Samuel L Braunstein, W J Munro, P van Loock, and G J Milburn. Quantum computation by communication. New Journal of Physics, 8(2):30, feb 2006.
- [29] Shapiro, Jeffrey H. Single-photon Kerr nonlinearities do not help quantum computation. Phys. Rev. A, 73:062305, Jun 2006.

- [30] Shapiro, Jeffrey H. and Bondurant, Roy S. Qubit degradation due to cross-phase-modulation photon-number measurement. Phys. Rev. A, 73:022301, Feb 2006.
- [31] **Gea-Banacloche, Julio**. Impossibility of large phase shifts via the giant Kerr effect with single-photon wave packets. Phys. Rev. A, 81:043823, Apr 2010.
- [32] He, Bing, Lin, Qing, and Simon, Christoph. Cross-Kerr nonlinearity between continuous-mode coherent states and single photons. Phys. Rev. A, 83:053826, May 2011.
- [33] He, Bing, MacRae, Andrew, Han, Yang, Lvovsky, A. I., and Simon, Christoph. Transverse multimode effects on the performance of photon-photon gates. Phys. Rev. A, 83:022312, Feb 2011.
- [34] Le, Dat Thanh, Asavanant, Warit, and An, Nguyen Ba. Heralded preparation of polarization entanglement via quantum scissors. Phys. Rev. A, 104:012612, Jul 2021.
- [35] Dat Thanh Le, Cao Thi Bich, and Nguyen Ba An. Feasible and economical scheme to entangle a polarized coherent state and a polarized photon. Optik, 225:165820, 2021.
- [36] Furusawa, Akira and Van Loock, Peter. Quantum teleportation and entanglement: a hybrid approach to optical quantum information processing. John Wiley & Sons, 2011.
- [37] Takeda, Shuntaro and Mizuta, Takahiro, Fuwa, Maria, van Loock, Peter, and Furusawa, Akira. Deterministic quantum teleportation of photonic quantum bits by a hybrid technique. Nature, 500(7462):315–318, 2013.
- [38] Andersen, Ulrik L., Neergaard-Nielsen, Jonas S., van Loock, Peter, and Furusawa, Akira. Hybrid discrete- and continuous-variable quantum information. Nature Physics, 11(9):713–719, 2015.
- [39] Gerry, Christopher C and Knight, Peter L. Introductory quantum optics. Cambridge university press, 2023.
- [40] Fan, Bixuan, Kockum, Anton F., Combes, Joshua, Johansson, Göran, Hoi, Io-chun, Wilson, C. M., Delsing, Per, Milburn, G. J., and Stace, Thomas M. Breakdown of the Cross-Kerr Scheme for Photon Counting. Phys. Rev. Lett., 110:053601, Jan 2013.

- [41] Shi, Tao, Chang, Darrick E., and Cirac, J. Ignacio. Multiphoton-scattering theory and generalized master equations. Phys. Rev. A, 92:053834, Nov 2015.
- [42] Joseph Kerckhoff Joshua Combes and Mohan Sarovar. The SLH framework for modeling quantum input-output networks. Advances in Physics: X, 2(3):784–888, 2017.
- [43] Gardiner, Crispin and Zoller, Peter. Quantum noise: a handbook of Markovian and non-Markovian quantum stochastic methods with applications to quantum optics. Springer, Berlin, 2004.
- [44] **Shanshan Xu**. Theory of few-photon quantum scattering in nanophotonic structures. PhD thesis, Stanford University, 2017.
- [45] Loudon, Rodney. The quantum theory of light. OUP Oxford, 2000.
- [46] Vinu, Athul and Roy, Dibyendu. Single photons versus coherent-state input in waveguide quantum electrodynamics: Light scattering, Kerr, and cross-Kerr effect. Phys. Rev. A, 107:023704, Feb 2023.

#### Dat Thanh Le

Analog Quantum Circuits Pty. Ltd. Brisbane Australia dat.le@aqcircuits.com

## Nguyen Ba An

Thang Long Institute of Mathematics and Applied Sciences Thang Long University, Nghiem Xuan Yem, Hoang Mai Hanoi Vietnam annb@thanglong.edu.vn